

We are IntechOpen, the world's leading publisher of Open Access books Built by scientists, for scientists

6,900

Open access books available

186,000

International authors and editors

200M

Downloads

Our authors are among the

154

Countries delivered to

TOP 1%

most cited scientists

12.2%

Contributors from top 500 universities



WEB OF SCIENCE™

Selection of our books indexed in the Book Citation Index
in Web of Science™ Core Collection (BKCI)

Interested in publishing with us?
Contact book.department@intechopen.com

Numbers displayed above are based on latest data collected.
For more information visit www.intechopen.com



Simulations of Yarn Unwinding from Packages

Stanislav Praček and Nace Pušnik

Abstract

Yarn unwinding from stationary packages has an important role in many textile processes. In order to achieve high unwinding velocity that can lead to increased production rate, it is necessary to develop packages with a suitable geometry, dimensions, and winding type. The optimal design of the package leads to an optimal form of the balloon and low and uniform tension at high unwinding speed. In this work I will show a simple mathematical model which can be used for simulating the unwinding process. Using experimental values I will find a relation between the angular velocity of the yarn around the axis and the tension. This will allow me to calculate the oscillations of the tension in the yarn during the unwinding from packages of different geometries and with different winding angles. I will find an optimal design for a package of a new generation.

Keywords: yarn unwinding, packages, parallel winding, cross winding, unwinding simulations, oscillations of the tension in yarn

1. Introduction

At the end of the production process of a spinning factory, yarn is wound on packages. Therefore, packages are a crucial intermediate product of textile industry. The rapid development of fast-running weaving and knitting machines has led to the situation where unwinding yarn from packages is one of the main production bottlenecks. For this reason it is of utmost importance to determine the package geometry and the winding angle which allow to maximize the unwinding velocity given the allowed highest yarn tension [1–6].

The yarn is being withdrawn with velocity V through an eyelet, where we also fix the origin O of our coordinate system (**Figure 1**). The yarn is rotating around the z axis with an angular velocity ω . At the lift-off point (L_p), the yarn lifts from the package and forms a balloon (the name stems from the fact that in one period of rotation, this part of the yarn describes a surface of evolution that has a form of a balloon). At the unwinding point (U_p), the yarn starts to slide on the surface of the package. Angle ϕ is the winding angle of the yarn on the package. In order to be able to compare various package designs, it is necessary to determine the influence of the winding angle of the package on the angular velocity of the yarn forming the balloon, since the angular velocity determines to a great extent the yarn tensions. The results of simulations will be used to suggest a design for packages of new generations, on which two kinds of layers would alternate: parallel-wound layers and layers with high unwinding angle.

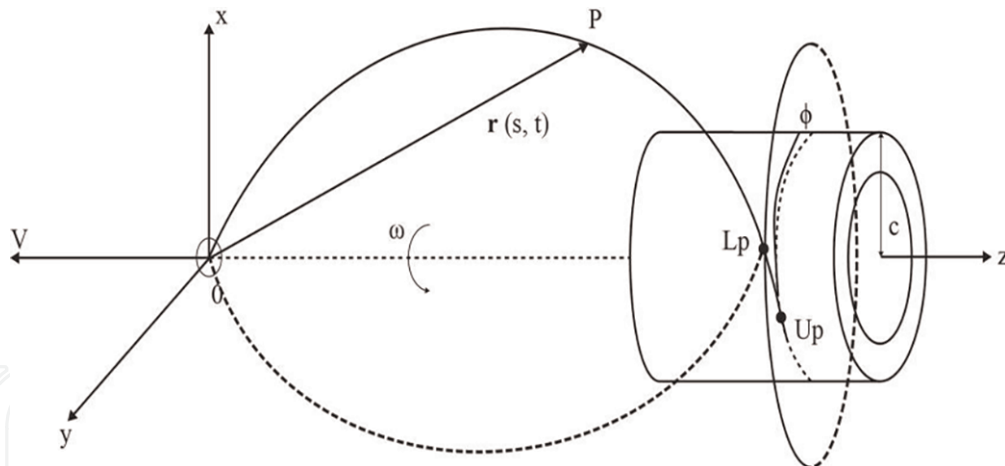


Figure 1.
Yarn unwinding from a cylindrical package.

2. Machines and materials

The current angular velocity ω for cylindrical packages is computed by using the relation [2, 3]

$$\omega = \frac{2\pi}{t} = \frac{V}{c} \frac{\cos \phi}{(1 - \sin \phi)}. \quad (1)$$

In order to perform simulations, we additionally need a relation between the unwinding velocity and the yarn tension. The tension is largest in the eyelet through which the yarn is being pulled [3].

We measured tension for parallel-wound cylindrical packages of different dimensions and for different unwinding velocities (**Table 1**). For such packages the winding angle is $\phi \sim 0^\circ$, and we obtain $\omega = V/c$. This is the expected result since in this case the unwinding velocity V equals the circumferential velocity of the lift-off point, which is given by $c\omega$ [3]. **Figure 2** shows the unwinding yarn system. Yarn is withdrawn from a fixed packages by a Lesson yarn drive at transport speed of up to 2000 m per minute. Support for the guide is fixed to which the sensor for measuring the tension of the yarn is installed.

Parameters	Range of values
Yarn type	Cotton
Yarn linear density m	0.8 g/m
Yarn titer tex	41.6 tex
Package radius c	92–110 mm
Package winding angle ϕ_0	5°
Package height mm	250 mm
Transport speed V	1000–2000 m/min

Table 1.
Experimental parameters.

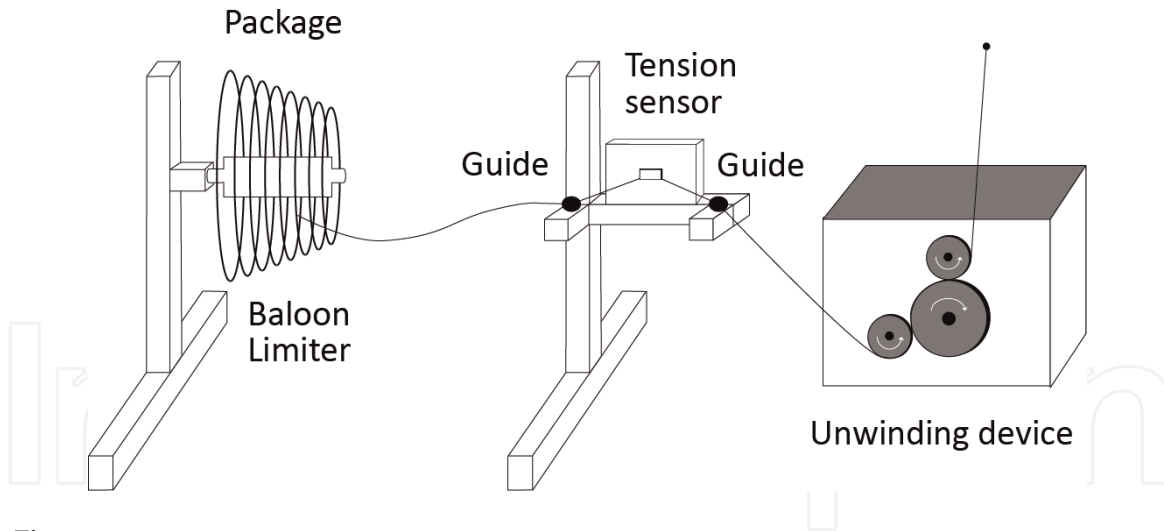


Figure 2.
 Setup of the unwinding system.

3. Methods and simulation

In a recent paper, we developed a mathematical model [7, 8]:

$$f(t) = \text{sign}(\sin t) |\sin t|^{\frac{1}{40}} \quad (2)$$

which would permit to simulate the process of unwinding (**Figure 3**).
 In our simulation we calculate the winding angle using the function

$$\phi_0(t) = \phi f(t) \quad (3)$$

where ϕ is the maximal angle of wind, then we determine the corresponding angular velocity ω , and finally we obtain an approximation for the tension using data from Section 2. In our calculations we considered unwinding for two consecutive layers of yarn, so that the package radius remains approximately constant during this time.

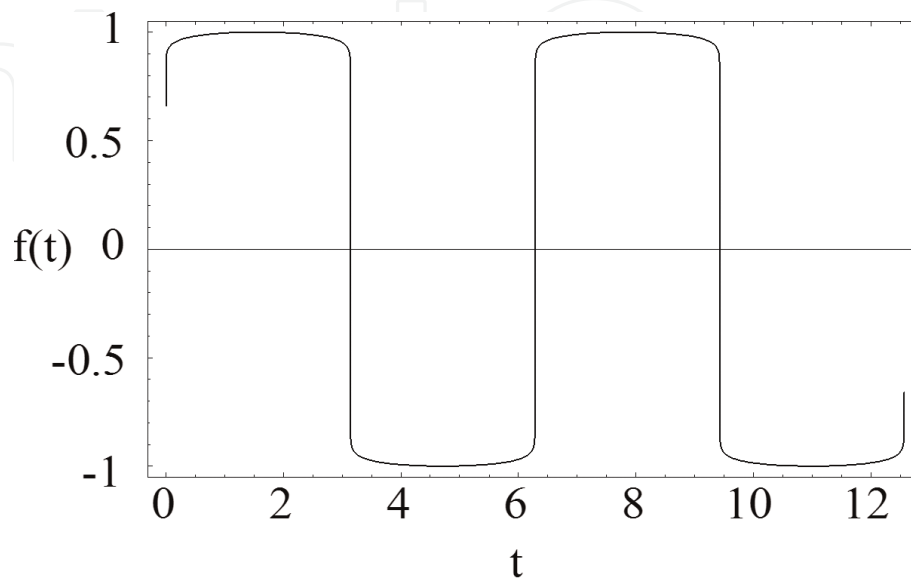


Figure 3.
 Model function for winding angle.

The graph below presents the changing tension in the yarn as we unwind yarn from a cylindrical package. The time is expressed in units of phase: 2π corresponds to one cycle of unwinding point up and down the package.

In **Figures 4** and **5**, we show the results for the oscillations of tension for a range of four winding angles $\phi \sim 0, 10, 20,$ and 30° for a very small package radius of $c = 70$ mm and for two different unwinding velocities, $V = 1000$ and 1400 m/min, respectively. The tension is a function of angular velocity, so it is oscillating in agreement with Eq. (1). When the direction of unwinding changes near the edges of the package, the yarn tension undergoes a rapid change. Such sudden jumps lead to strong strain in the yarn, and the yarn can be damaged or even broken in two parts. In this case we again observe very high tension in the yarn for all the enumerated winding angles. The tension oscillates from 0.05 to 1.8 N. In such case, the unwinding would fail.

Figure 6 shows the time dependence of the yarn tension for unwinding velocity of $V = 2000$ m/min. The winding angle is fixed at $\phi_0 = 5^\circ$, and we consider package radii in the range from $c = 70$ to 500 mm. For large package radius, the tension is small, but it becomes sizable already at rather low radius between $c = 100$ and 200 mm. Nevertheless, the highest calculated tensions remain rather low, $T_0 = 0.7$ and 1.4 N.

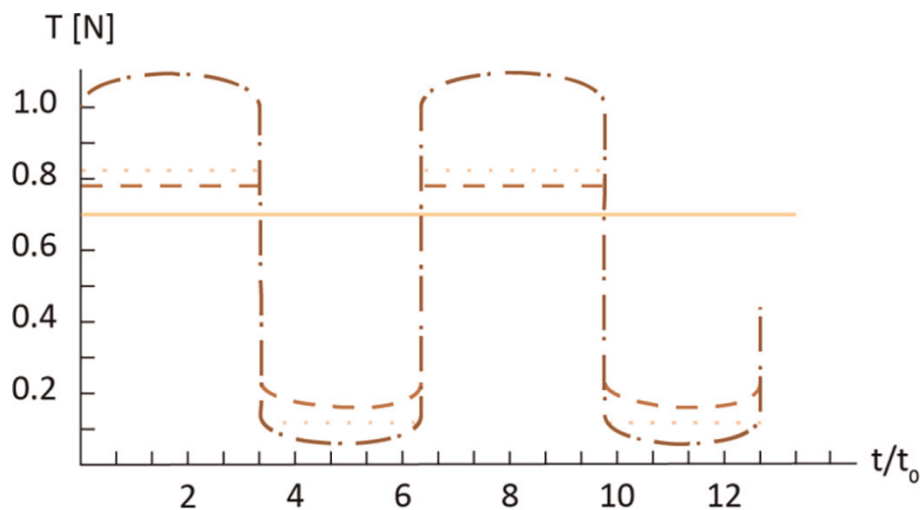


Figure 4.

Variation of the tension T_0 during the unwinding of the yarn from a cylindrical package for different winding angles. $V = 1000$ m/min, $c = 70$ mm. $\phi \sim 0^\circ$ (full line), $\phi = 10^\circ$ (dashed line), $\phi = 20^\circ$ (dotted line), and $\phi = 30^\circ$ (dot-dashed line).

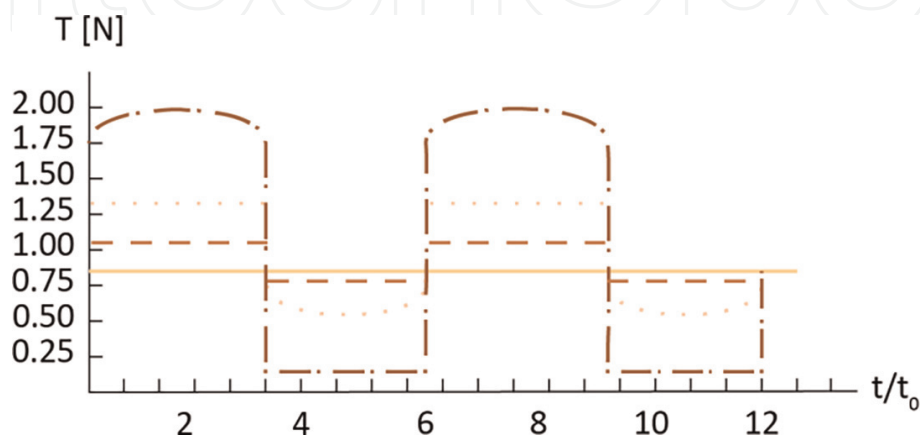


Figure 5.

Variation of the tension T_0 during the unwinding of the yarn from a cylindrical package for different winding angles. $V = 1400$ m/min, $c = 70$ mm. $\phi \sim 0^\circ$ (full line), $\phi = 10^\circ$ (dashed line), $\phi = 20^\circ$ (dotted line), and $\phi = 30^\circ$ (dot-dashed line).

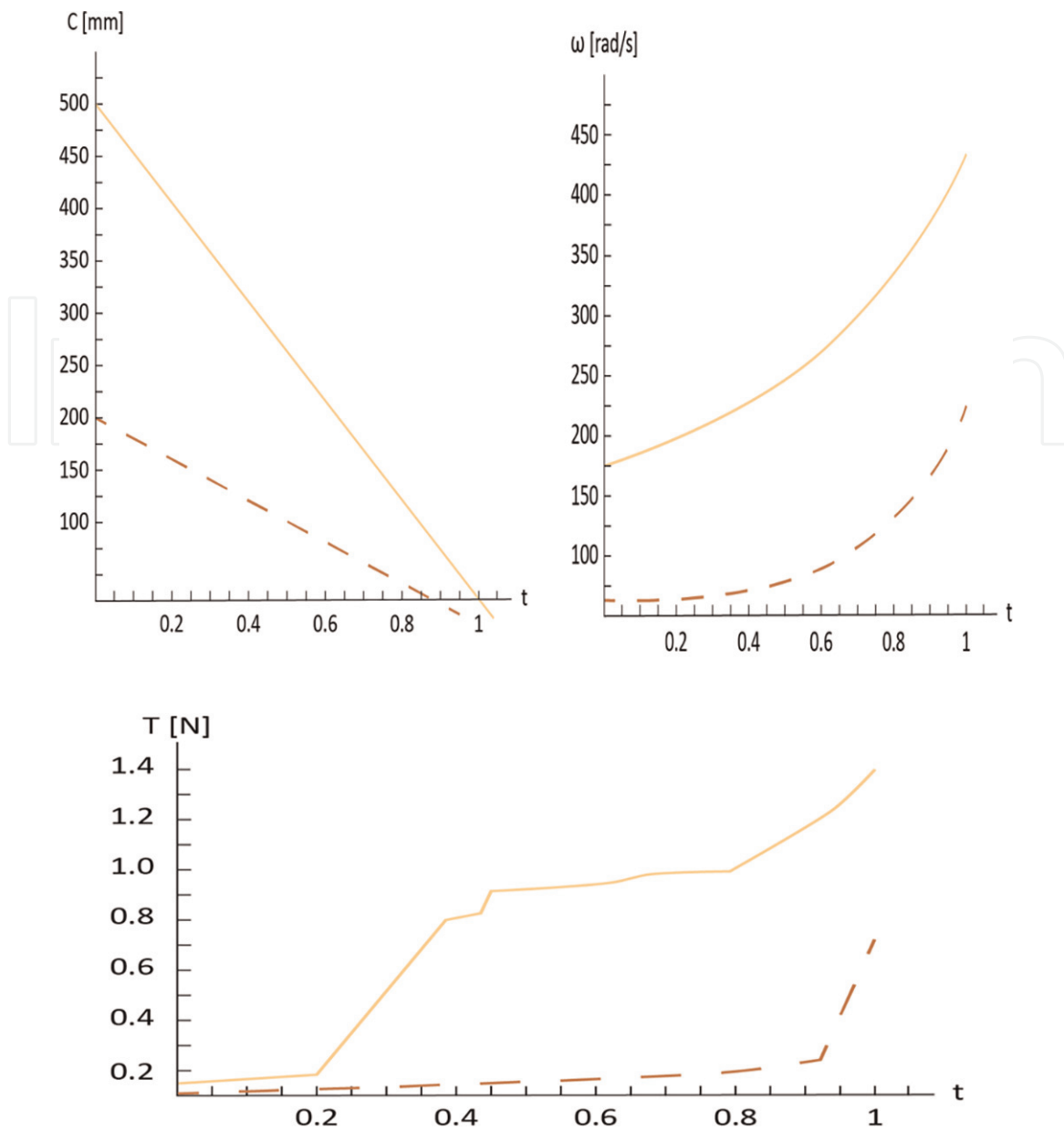


Figure 6.
 Variation of the parameters during the unwinding from a package at $V = 2000 \text{ m/min}$

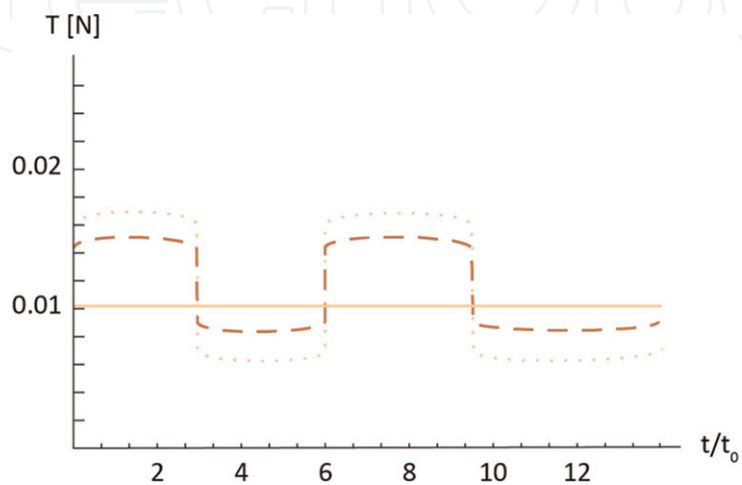


Figure 7.
 Comparison of the tension variation at different radii and winding angles. $V = 2000 \text{ m/min}$. The package radii is $c = 500 \text{ mm}$. Winding angles: $\phi \sim 0^\circ$ (full line), $\phi = 5^\circ$ (dashed line), and $\phi = 10^\circ$ (dotted line).

We therefore make the following important conclusion: the yarn tension can be strongly reduced by making use of packages with large radius.

The variation of the radius of the topmost layer, the angular velocity, and the tension in the yarn during the unwinding from a parallel-wound cylindrical package at $V = 2000$ m/min, $\phi = 5^\circ$, $c = 70\text{--}200$ mm (dashed line), and $c = 160\text{--}500$ mm (full line).

In **Figures 7–10**, we compare the time dependence of the yarn tension for two package radii, $c = 500$ and 160 mm, and for three winding angles 0 , 5 , and 10° at two unwinding velocities, $V = 2000$ and 1500 m/min. For package radii 500 mm, we find suitable tensions $T = 0.015$ and $0.03\text{--}0.04$ N for all winding angles. For package radius 160 mm, we find acceptable tension only for winding angles $\phi \sim 0$

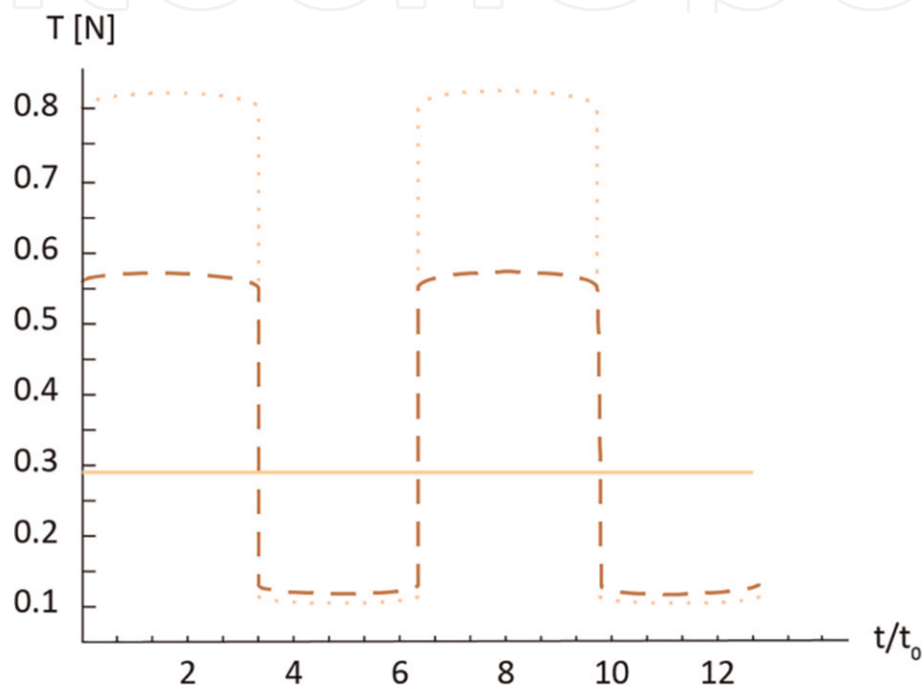


Figure 8.

Comparison of the tension variation at different radii and winding angles. $V = 2000$ m/min. The package radii is $c = 160$ mm. Winding angles: $\phi \sim 0^\circ$ (full line), $\phi = 5^\circ$ (dashed line), and $\phi = 10^\circ$ (dotted line).

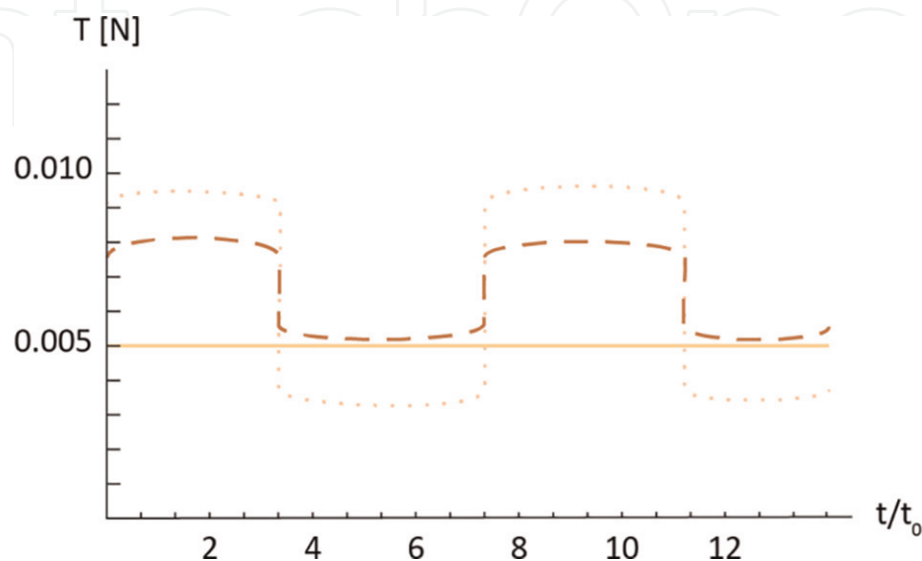


Figure 9.

Comparison of the tension variation at different radii and winding angles. $V = 1500$ m/min. The package radii is $c = 500$ mm. Winding angles: $\phi \sim 0^\circ$ (full line), $\phi = 5^\circ$ (dashed line), and $\phi = 10^\circ$ (dotted line).

and $\phi = 5^\circ$: in these cases the tension rises at most to 0.055 N, which is at the higher end of the acceptable values. At $\phi = 10^\circ$ we observe tensions around 0.08 N, which exceeds the limit.

Figures 11–13 show the dependence of the amplitude of tension oscillations as a function of the package radius (from 70 to 500 mm) and winding angle (from 0 to 20°) for three different unwinding velocities: 1000, 1500, and 2000 m/min. For all unwinding velocities, the oscillation amplitudes are larger for packages with smaller radius and large winding angle. In particular, the oscillations are very large for radii lower than 160 mm and for winding angles exceeding 5° .

The oscillations of yarn tension are related to the variation of the angular velocity of yarn rotation around the package axis.

The amplitude of the angular velocity oscillation is

$$\Delta\omega = \omega_{\max} - \omega_{\min} = \frac{2V}{c} \tan \phi \quad (4)$$

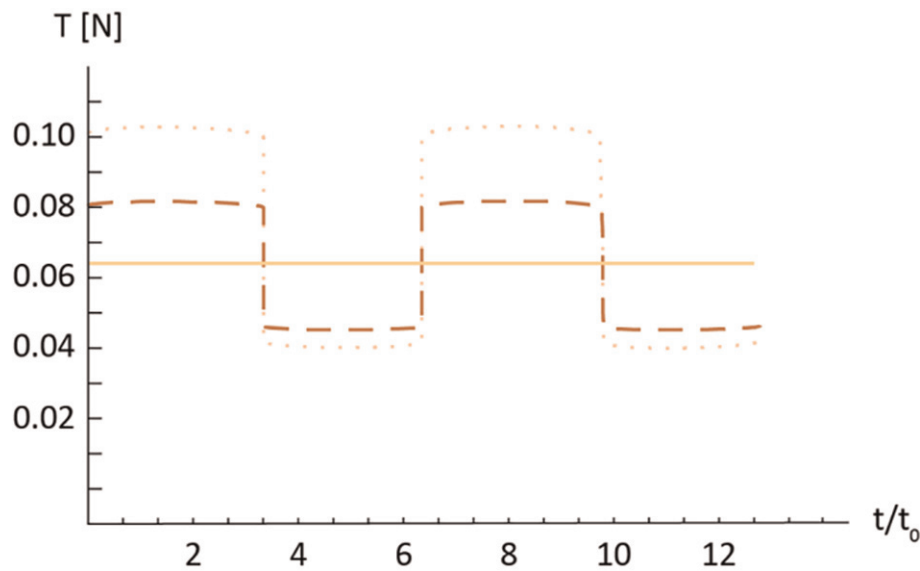


Figure 10. Comparison of the tension variation at different radii and winding angles. $V = 1500$ m/min. The package radii is $c = 160$ mm. Winding angles: $\phi \sim 0^\circ$ (full line), $\phi = 5^\circ$ (dashed line), and $\phi = 10^\circ$ (dotted line).

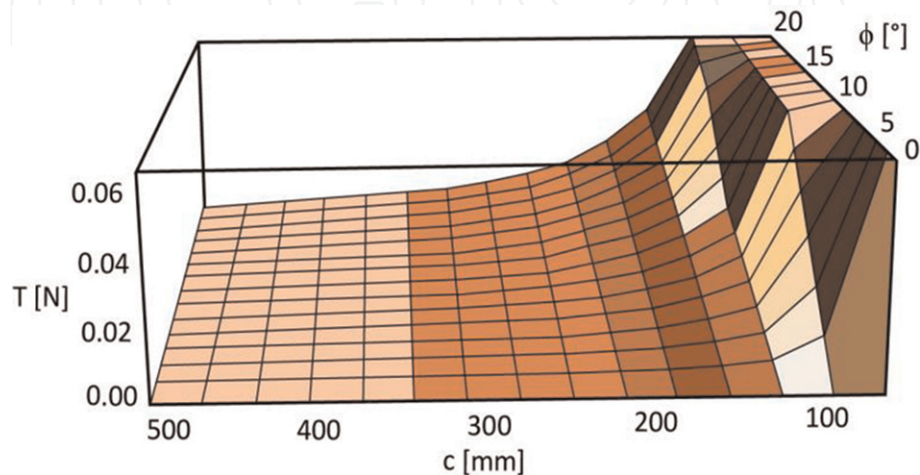


Figure 11. Comparison of the amplitude of the tension oscillation as a function of the package radius c and the winding angle ϕ for constant unwinding velocity $V = 1000$ m/min.

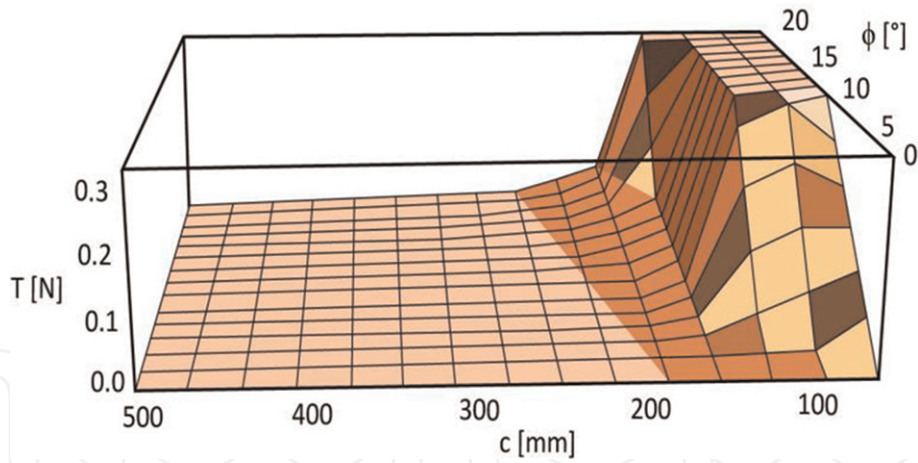


Figure 12.
Comparison of the amplitude of the tension oscillation as a function of the package radius c and the winding angle ϕ for constant unwinding velocity $V = 1500$ m/min.

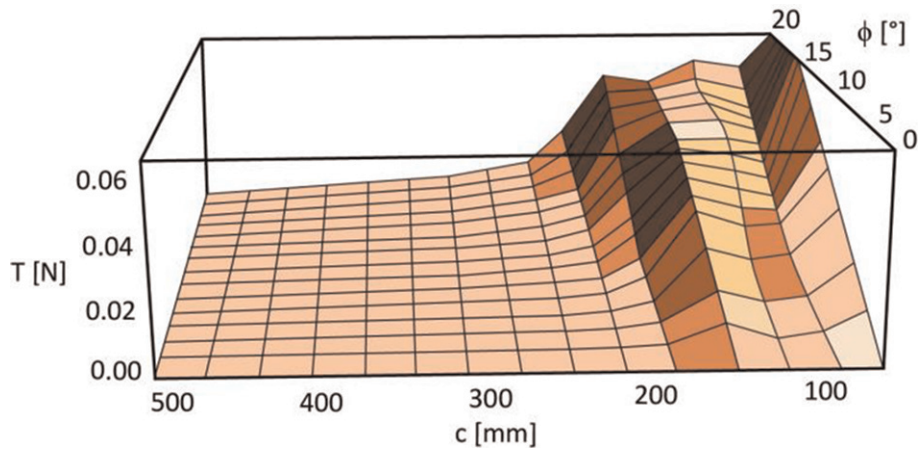


Figure 13.
Comparison of the amplitude of the tension oscillation as a function of the package radius c and the winding angle ϕ for constant unwinding velocity $V = 2000$ m/min.

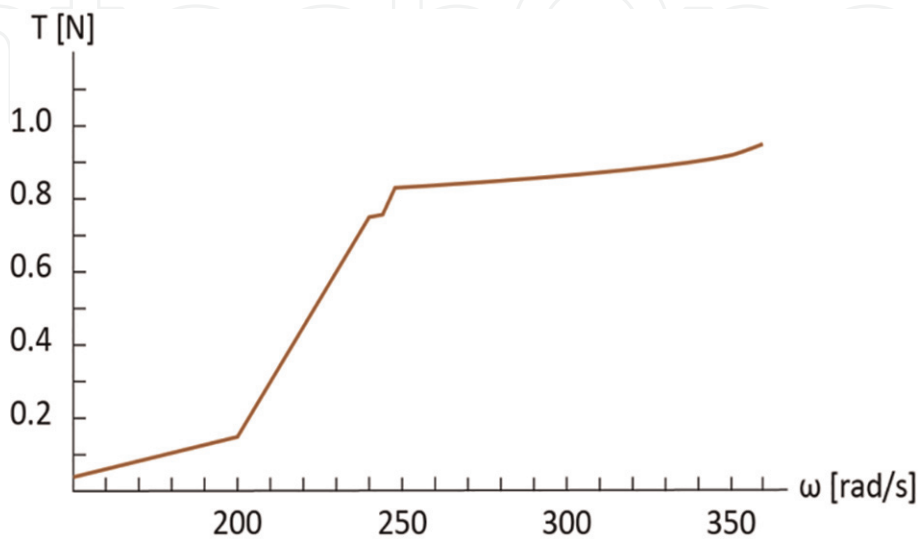


Figure 14.
Dependence of tension T on angular velocity ω of the yarn.

In the region of interest, i.e. for $\phi < 25^\circ$, we have $\tan \phi \sim \phi$.
 We get

$$\Delta\omega \approx \frac{2V\phi}{c}. \quad (5)$$

This means that the amplitude of the angular velocity oscillation is approximately proportional to the unwinding velocity and winding angle, but inversely proportional to the package radius.

From this relation we can estimate the yarn tension oscillation, knowing the dependence between the angular velocity and the tension that can be experimentally measured. We can also make use of **Figure 14**, which can serve to roughly estimate the amplitude of oscillations. We determine the average angular velocity during unwinding through

$$\omega_0 = \frac{(\omega_{\max} + \omega_{\min})}{2} = \frac{V}{c} \frac{1}{\cos \phi} \approx \frac{V}{c}. \quad (6)$$

Here we made use of the small-angle approximation $\cos(\phi) \approx 1$. This relation is applicable in the same range as the expansion for the tan function, and the error is also of the same magnitude.

In **Figure 14** we determine the interval from $\omega_0 - \Delta\omega/2$ to $\omega_0 + \Delta\omega/2$ and read off the interval of yarn tension it corresponds to. The amplitude of yarn tension oscillations is then simply the difference between the maximal and minimal values.

This graphical method for making estimations can be applied to better understand **Figure 15**, where we plot the dependence of the oscillation amplitude on the package radius for winding angle $\phi = 10^\circ$ and unwinding velocity $V = 2000$ m/min. This is, in fact, a section of **Figure 13** at constant angle ϕ . As a rough rule, the amplitude of the oscillations decreases with increasing package radius c . In addition,

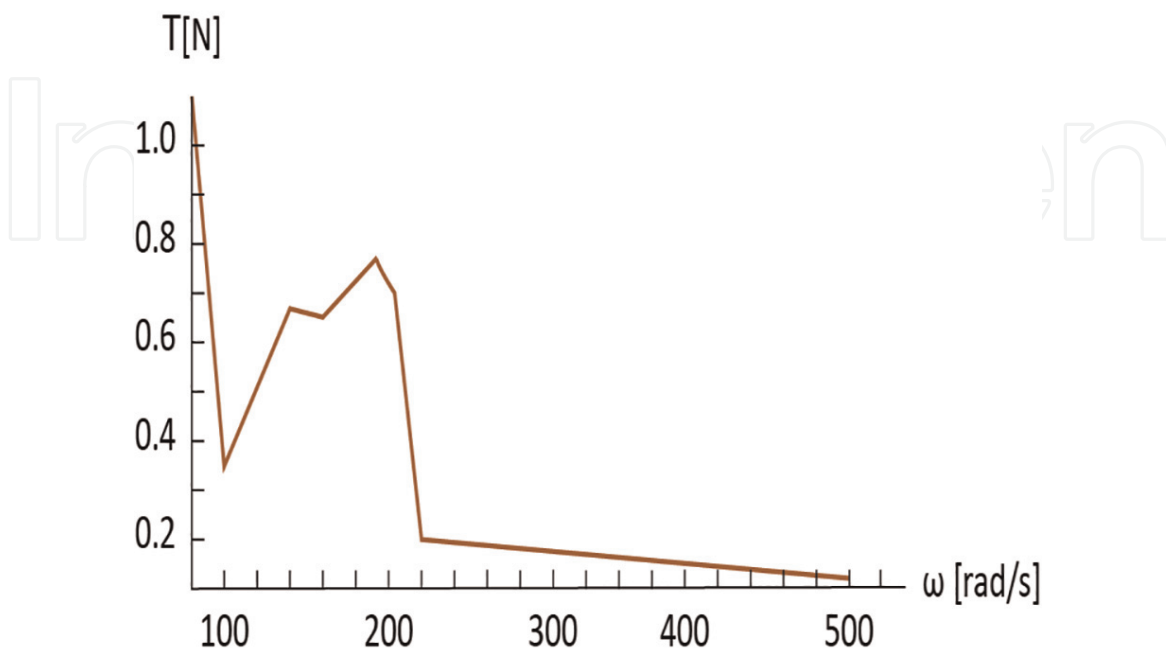


Figure 15.
 Cross section of the plot at $\phi = 10^\circ$.

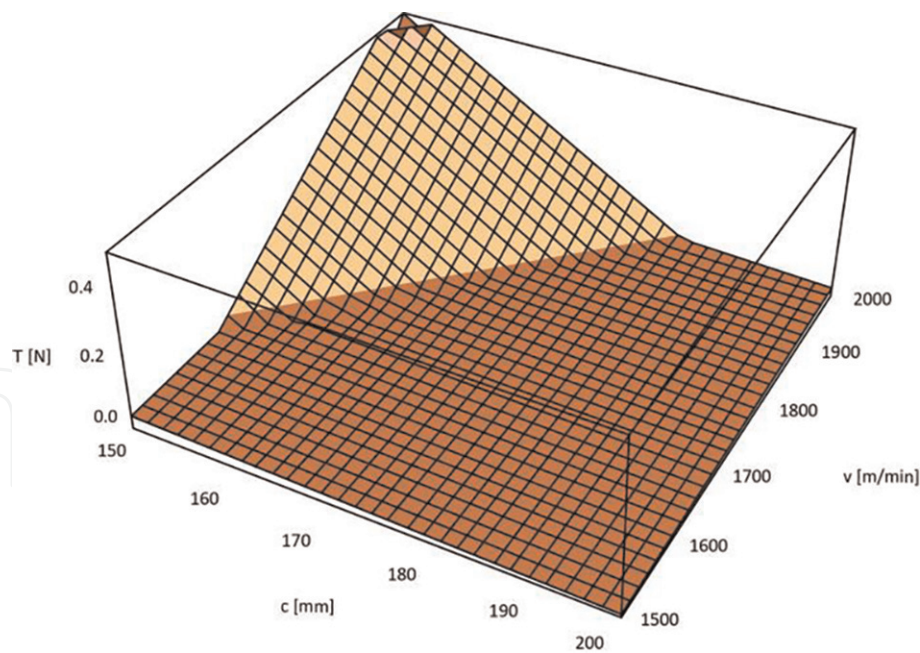


Figure 16.

Comparison of the amplitude of the tension oscillation as a function of the unwinding velocity V and the package radius c . The winding angle is constant, $\phi = 5^\circ$.

however, one observes a peak in the range of radii from $c = 110$ to 180 mm. This is due to the particular dependence of the tension on the angular velocity, as shown in **Figure 14**. In some ranges of ω , this dependence is steeper, for instance, from $\omega = 200$ to 240 rad/s. In this interval, oscillations of angular velocity lead to large amplitude of tension oscillations. In other ranges, for instance, from $\omega = 250$ to 300 rad/s, the tension does not depend much on the angular velocity; hence the yarn tension oscillations are small.

The cross section of the previous figure at the winding angle $\phi = 10^\circ$.

In **Figure 16** we plot the dependence of tension oscillation amplitude from the package radius and unwinding velocity at constant winding angle $\phi = 5^\circ$. We notice that the lines of constant amplitude are simply straight lines. This means that the amplitude of tension oscillations at constant angle depends only on V/c , as expected from Eqs. (4) and (5). This suggests the possibility to make a compromise: if it is known that the yarn is damaged at some given amplitude of tension oscillations, then the possible choices of package radius c and unwinding velocity V lie on a straight line. One can thus use small package radii with small unwinding velocities or large packages with correspondingly higher unwinding velocities. It is also apparent that during unwinding from packages with a radius of 150 mm, it is possible to unwind at all velocities shown with a possible exception of those near the maximum values of $V = 2000$ m/min.

4. Packages with alternating layers

To reduce the tension oscillations, we devised packages of alternating layers. They are constructed so that:

- a. When unwinding point moves backwards, the parallel layers are being unwound.
- b. When unwinding point moves forward, the layers with high winding angle are being unwound. Between two parallel layers, there should always be one layer with higher winding angle in order to avoid interweaving of parallel layers.

In **Figures 17 and 18**, we compare packages with alternating layers with regular cross-wound packages. The unwinding velocity is $V = 2000$ m/min for two package radii $c = 200$ and 150 mm. The winding angle of cross-wound layers is $\phi = 10^\circ$. As expected, the packages with alternating parallel-wound and cross-wound layers significantly reduce the tension. We have thus achieved an elimination of high tension spikes which lead to yarn breaking in conventional cross-wound packages. For this reason, the new-generation packages would allow unwinding at higher velocities than traditional packages.

In **Figures 19–21**, we compare the amplitude of the yarn tension oscillation in regular cross-wound packages and in new-generation packages for different unwinding velocities from $V = 1000$ to 2000 m/min and for different winding angles, from $\phi = 0$ to 20° . Package radii are 120 , 150 , and 200 mm. The amplitude of tension oscillation is larger for large unwinding velocities and for larger winding angles. This is the case for all package radii. The totality of the results indicates that this dependence is significantly larger for conventional cross-wound packages,

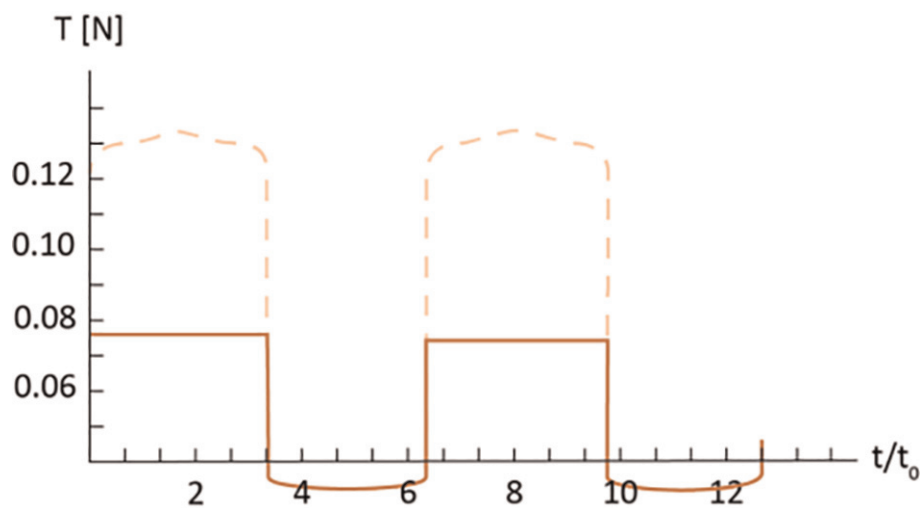


Figure 17. Comparison of the tension variation during the unwinding of the yarn from conventional cross-wound packages (dashed line) and from new-generation packages with alternating layers (solid line). Unwinding velocity $V = 2000$ m/min, package radius $c = 200$ mm, and winding angle $\phi = 10^\circ$.

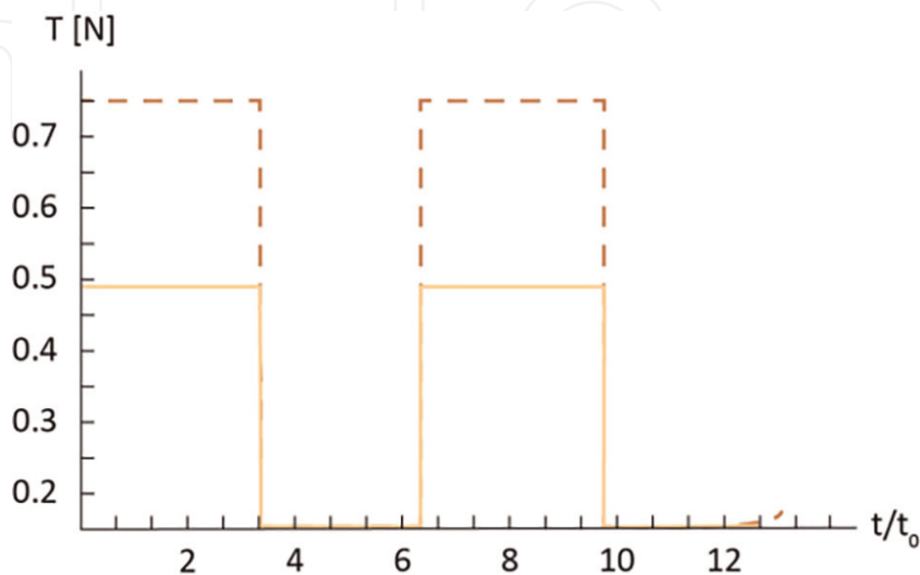


Figure 18. Comparison of the tension variation during the unwinding of the yarn from conventional cross-wound packages (dashed line) and from new-generation packages with alternating layers (solid line). Unwinding velocity $V = 2000$ m/min, package radius $c = 150$ mm, and winding angle $\phi = 10^\circ$.

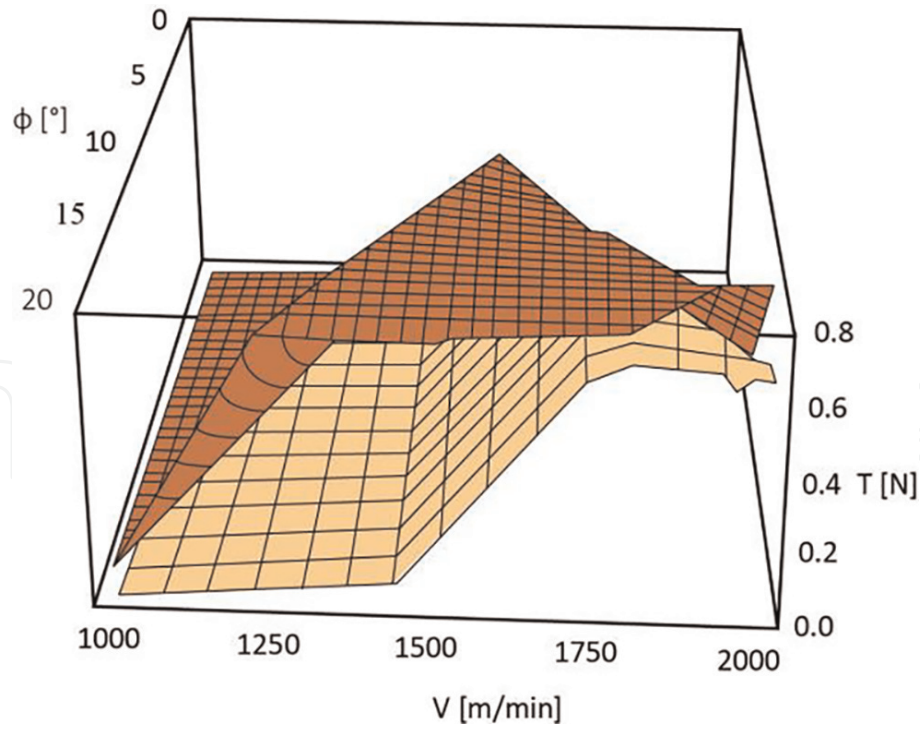


Figure 19. Comparison of the amplitude of the tension oscillation in packages with alternating layers (lighter) and in conventional cross-wound packages (darker). Package radius in both cases is $c = 120$ mm.

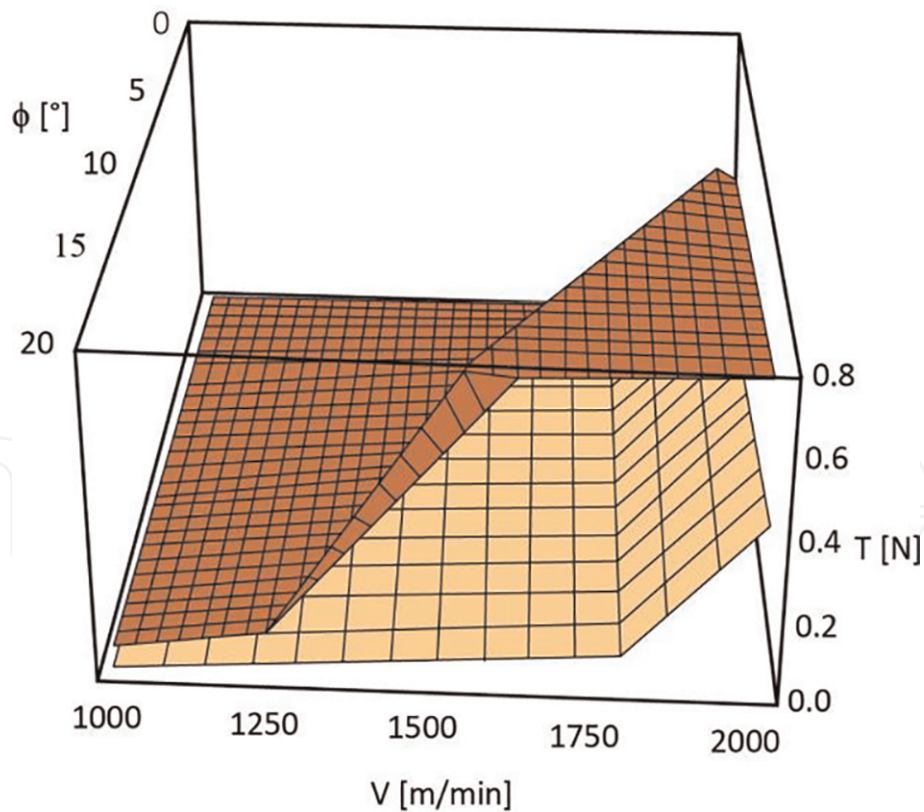


Figure 20. Comparison of the amplitude of the tension oscillation in packages with alternating layers (lighter) and in conventional cross-wound packages (darker). Package radius in both cases is $c = 150$ mm.

where the oscillation amplitude becomes very large, while the oscillations are notably lower in the new-generation packages. The differences are largest for the package radius of $c = 200$ mm, where the difference at unwinding velocity of

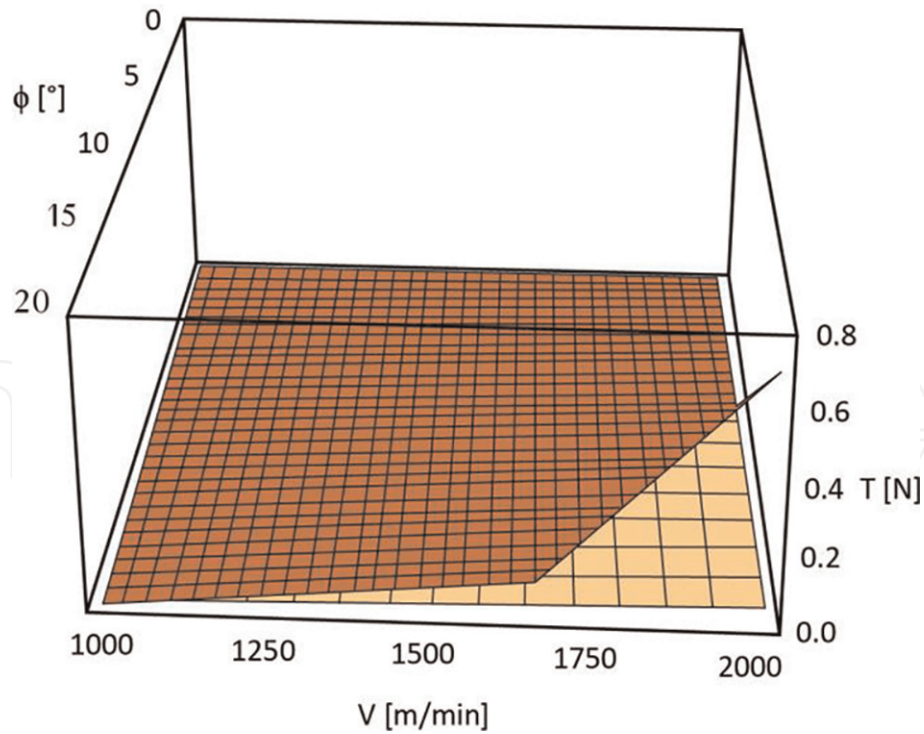


Figure 21. Comparison of the amplitude of the tension oscillation in packages with alternating layers (lighter) and in conventional cross-wound packages (darker). Package radius in both cases is $c = 200$ mm.

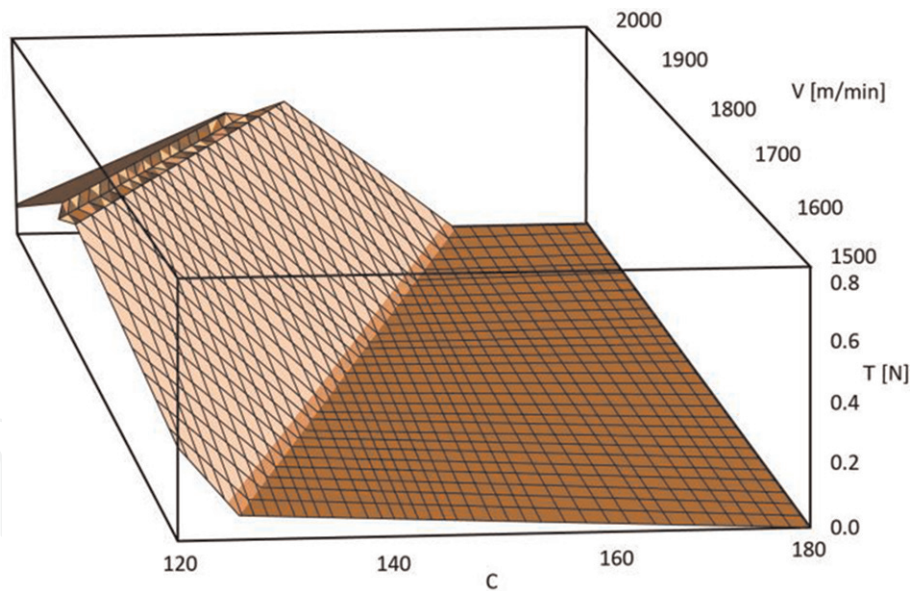


Figure 22. Amplitude of the tension oscillations in packages with alternating layers as a function of the unwinding velocity ranges from $V = 1500$ to 2000 m/min, and the package radius ranges from $c = 120$ to 180 mm. Winding angle $\phi = 10^\circ$.

$V = 2000$ m/min equals 0.65 N. At package radius of $c = 150$ mm, this difference is still 0.4 cN.

In **Figures 22** and **23**, we show the amplitude of the tension oscillations in new-generation packages as a function of package radius and unwinding velocity at constant winding angle of cross-wound layers of $\phi = 10^\circ$. The first figure suggests that at $V = 2000$ m/min, the package radius should be at least $c = 150$ mm in order to avoid yarn breaking.

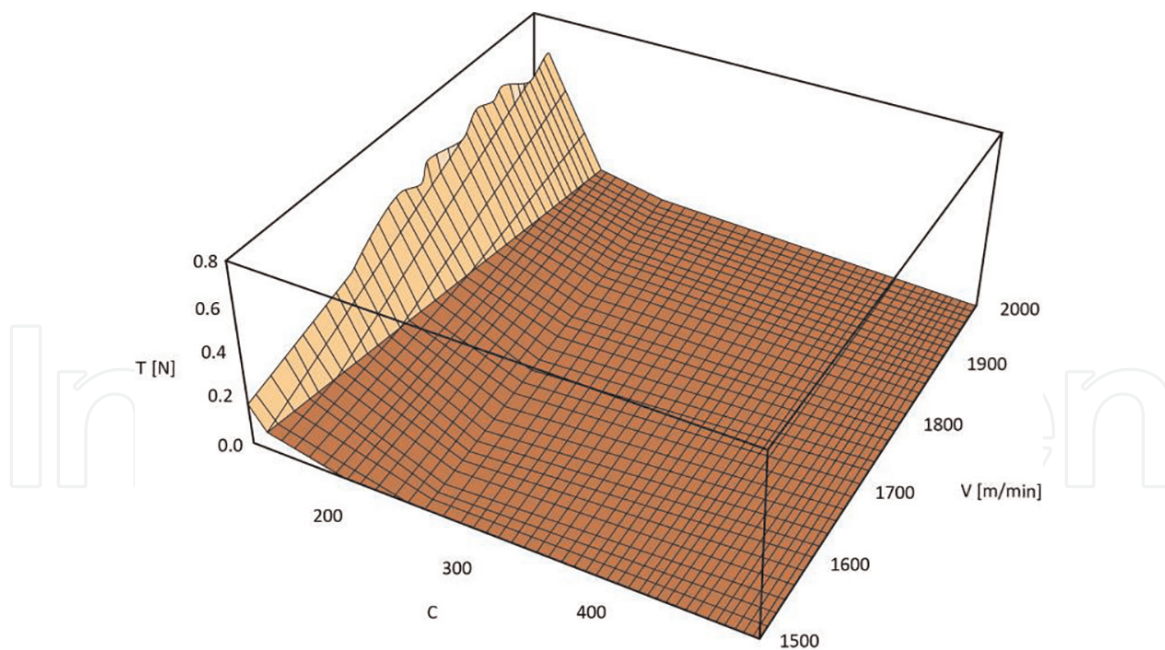


Figure 23.

Amplitude of the tension oscillations in packages with alternating layers as a function of the unwinding velocity ranges from $V = 1000$ to 2000 m/min, and the package radius ranges from $c = 120$ to 500 mm. Winding angle $\phi = 10^\circ$.

5. Conclusion

The problem of high yarn tension and its high oscillations can be avoided by constructing packages of new generations. From this study, the following conclusions can be drawn:

- In designing new package times, it is desirable to limit the maximal value of the tension in yarn but also the amplitude of the tension oscillations.
- The yarn tension can be strongly reduced by making use of packages with large radius.
- The alternating design helps to reduce sudden change of tension, and it leads to higher stability of the unwinding process.

With this design tension and the amplitude of the tension oscillations can be significantly reduced. In this case it is possible to safely unwind from packages of smaller radius even at higher unwinding velocities. This would allow higher production rates without increased downtime due to yarn breaking. Based on the results of our calculations, we propose a package with the following characteristics: the inner cylinder radius should be 150 mm (arguably even 100 or 120 mm), and the outer package radius should be from 400 to 500 mm. Parallel layers should have a winding angle that is as close to 0 as possible, while the winding angle of other layers should be no higher than 10° .

IntechOpen

IntechOpen

Author details

Stanislav Praček* and Nace Pušnik
Faculty of Natural Sciences and Engineering, University of Ljubljana, Ljubljana,
Slovenija

*Address all correspondence to: stane.pracek@ntf.uni-lj.si

IntechOpen

© 2019 The Author(s). Licensee IntechOpen. This chapter is distributed under the terms of the Creative Commons Attribution License (<http://creativecommons.org/licenses/by/3.0>), which permits unrestricted use, distribution, and reproduction in any medium, provided the original work is properly cited. 

References

[1] Kothari VK, Leaf GAV. The unwinding of yarns from packages. Part I: The theory of yarn-unwinding. *Journal of the Textile Institute*. 1979;3:89-95. DOI: 10.1080/00405007908631523

[2] Kothari VK, Leaf GAV. The unwinding of yarns from packages. Part II: Unwinding from cylindrical packages. *Journal of the Textile Institute*. 1979;3:96-104. DOI: 10.1080/00405007908631523

[3] Fraser WB, Ghosh TK, Batra SK. On unwinding yarn from cylindrical package. *Proceedings of the Royal Society of London*. 1992;436:479-498. DOI: 10.1080/rspa.1992.0030

[4] Fraser WB. The effect of yarn elasticity on an unwinding ballon. *The Journal of The Textile Institute*. 1992;83:603-613. DOI: 10.1080/00405009208631235

[5] Kong XM, Rahn CD, Goswami BC. Steady-state unwinding of yarn from cylindrical packages. *Textile Research Journal*. 1999;69(4):292-306. DOI: 10.1177/00405175990690040

[6] Clark JD, Fraser WB, Sharma R, Rahn CD. The dynamic response of a ballooning yarn: Theory and experiment. *Proceedings of the Royal Society of London*. 1998;A454:2767-2789. DOI: 10.1098/rspa.1998.0280

[7] Praček S. Theory of string motion in the textile process of yarn unwinding. *International Journal of Nonlinear Sciences and Numerical Simulation*. 2007;8(3):451-460. DOI: 10.1515/IJNSNS.2007.8.3.415

[8] Pušnik N, Praček S. The effect of winding angle on unwinding yarn. *Transactions of FAMENA*. 2016;40(3):29-42. DOI: 10.21278/TOF.40303. ISSN 1333-1124